and cones. However, more accurate results could be obtained for blunt-nosed bodies.

8) For cones used as decelerators, large drag reductions can be realized due to the wake-like nonuniform freestreams.

References

[1] Campbell, J. F. and Graw, J. W., "Experimental Flow Properties in the Wakes of a 120° Cone at Mach Number 2.20," TN D-5365, July 1969, NASA.

[2] Charczenko, N. and McShera, J. T., "Aerodynamic Characteristics of Towed Cones Used as Decelerators at Mach Numbers from 1.57 to 4.65," TN D-994, 1961, NASA.

[3] Coats, J. D., "Static and Dynamic Testing of Conical Decelerators for the Pershing Re-Entry Vehicle," AEDC-TN-60-188, U.S. Air Force, Oct. 1960, Arnold Engineering Development Center, Tullahoma, Tenn.

[4] McShera, J. T., "Aerodynamic Drag and Stability Characteristics of Towed Inflatable Decelerators at Supersonic Speeds," TN D-1601, 1963, NASA.

[5] Reding, J. P. and Ericsson, L. E., "Loads on Bodies in Wakes," *Journal of Spacecraft and Rockets*, Vol. 4, No. 4, April 1967, pp. 511–518.

[6] "Performance of and Design Criteria for Deployable Aerodynamic Decelerators," ASD-TR-61-579, Dec. 1963, NASA.

[7] Moore, F. G., "Calculation of Nonuniform Flow Fields Over Wedges and Cones by the Method of Characteristics," MS-thesis, 1968, Virginia Polytechnic Inst., Blacksburg, Va.

[8] Nerem, R. M., "Pressure and Heat Transfer on High-Speed Aerodynamic Decelerators of the Ballute Type," *AIAA Aerodynamic Deceleration Systems Conference*, AIAA, New York, 1966.

[9] Sullivan, R. P., Donaldson, C. duP., and Hayes, W. D., "Linearized Pressure Distribution with Strong Supersonic Entropy Layers," *Journal of Fluid Mechanics*, Vol. 16, 1963, pp. 481–496.

[10] George, A. R., "Perturbations of a Plane and Axisymmetric Entropy Layers," *AIAA Journal*, Vol. 5, No. 12, Dec. 1967, pp. 2155–2159.

[11] Brooks, E. N., "Application of the Method of Integral Relations to Supersonic Nonuniform Flow Past Wedges and Cones," M. S. thesis, 1967, Virginia Polytechnic Inst., Blacksburg, Va.

[12] South, J. C., Jr., "Calculation of Axisymmetric Supersonic Flow Past Blunt Bodies with Sonic Curves, Including a Program Description and Listing," TN D-4563, 1968, NASA.

[13] Barteneu, D. A. and Shishou, V. P., "Calculation of a Nonuniform Supersonic Axisymmetric Gas Flow Past a Pointed Body of Revolution," *Aviatsionnaia Tekhnika*, No. 1, 1968, pp. 3–9.

[14] Inouye, M., "Numerical Solutions for Blunt Axisymmetric Bodies in a Supersonic Spherical Source Flow," TN D-3383, 1966, NASA.

[15] Patterson, J. L. and Lewis, A. B., "An Investigation of Nonuniform Hypersonic Free-Stream Flows About Blunt Axisymmetric Bodies," AFFDL-TR-69-57, Nov. 1969, Air Force Flight Dynamics Lab., Wright-Patterson Air Force Base, Ohio.

[16] Shapiro, A. H., *The Dynamics and Thermodynamics of Compressible Fluid Flow*, Vols. I and II, Ronald Press, New York, 1953, pp. 516–522 and 676–688.

[17] Truitt, R. W., *Hypersonic Aerodynamics*, Ronald Press, New York, 1959, Chap. 1.

[18] Sims, J. L., "Tables for Supersonic Flow Around Right Circular Cones at Zero Angle of Attack," SP-3004, 1964, NASA.

[19] Love, E. S., "Generalized-Newtonian Theory," *Journal of the Aerospace Sciences*, Vol. 26, No. 5, 1959, pp. 314–315.

[20] Blottner, F. G., "Finite-Difference Methods of Solution of the Boundary-Layer Equations," *AIAA Journal*, Vol. 8, No. 2, Feb. 1970, pp. 193–205.

[21] Rakich, J. V., "Three-Dimensional Flow Calculation by the Method of Characteristics," *AIAA Journal*, Vol. 5, No. 10, Oct. 1967, pp. 1906–1908.

DECEMBER 1971 J. SPACECRAFT VOL. 8, NO. 12

Shock-Capturing, Finite-Difference Approach to Supersonic Flows

PAUL KUTLER* AND HARVARD LOMAX†
NASA Ames Research Center, Moffett Field, Calif.

Three-dimensional, inviscid, supersonic flow containing primary and embedded shock and expansion waves is determined over and behind simple wings and wing-body combinations. The nonlinear gas-dynamic equations are differenced according to a method proposed by MacCormack which is a variation of the Lax-Wendroff technique. Progressive development toward aircraftlike configurations is made by obtaining results for the flow over cones at large incidences, conical wing-body combinations, the flow over and behind pointed ogives, cone-cylinders, and planar delta wings at angle of attack. Comparisons are made with other applicable theories and when possible with experiment.

Introduction

MANY numerical techniques used to compute supersonic flowfields about simplified configurations have been developed in recent years. These techniques are based on both the Eulerian and Lagrangian systems and their combination. No attempt is made here to mention them all or to weigh their individual merits; rather, a few of them are referenced in order to bring out a perspective for the one particular approach that was used to compute all of the cases shown in the main body of this paper. The objective is to show that this one simple, rapid, and easily applied method can be used as a "production tool" to generate accurate solutions for the flow over and behind a wide variety of wings, bodies, and wing-body combinations with surrounding and embedded shock-waves.

Two distinct approaches are used in practice to compute multishocked flows. One is referred to as a sharp-shock technique and the other as a shock-capturing technique. Sharp-shock techniques isolate all shock waves by some logical procedure and apply the Rankine-Hugoniot shock relations

Presented as Paper 71-99 at the AIAA 9th Aerospace Sciences Meeting, New York, January 25–27, 1971; submitted February 8, 1971; revision received July 19, 1971.

* Research Scientist. Member AIAA.

† Chief, Computational Fluid Dynamics Branch. Member AIAA.

across them to identify their strength. Shock-capturing techniques, on the other hand, advance the initial data through a fixed Eulerian mesh, applying boundary conditions only at the body and in the free stream. Shock and expansion waves must form and decay automatically without special treatment of any kind.

The acceptance of shock-capturing numerical methods is far from universal, the principal objections being their inability to resolve the shock location with absolute precision, and their tendency to give spurious fluctuations for the magnitudes of the dependent variables in the vicinity of the shock. The purpose of this paper is to show by examples what can be expected when second-order, shock-capturing methods are used to compute the supersonic flow about two- and three-dimensional aerodynamic objects. The first few sections of this paper introduce the governing equations and the differencing scheme used to solve them and also describe a series of results obtained by a shock-capturing technique for relatively simple aerodynamic shapes, such as cones at angle of attack, pointed ogives, and cone-cylinders. These are compared with results from other methods and with experiment; they provide a basis for establishing the reliability of the proposed method. The later sections are concerned with flow about a conical wing-body combination having angle of attack and dihedral, and the flow surrounding and trailing a lifting supersonic-edged delta wing. The majority of computations were performed on an IBM 360/67 linked with a cathode ray display tube (CRT). The CRT, which possesses man-machine interaction capability, was used to study the flow field as it developed and to control any numerical instabilities that evolved.

Generalized Flow Equations

The gasdynamic equations for steady inviscid flow of a non-heat-conducting, perfect gas can be written in dimensionless, conservation law form for a generalized orthogonal coordinate system as follows:

$$\mathbf{E}_\zeta + \mathbf{F}_\eta + \mathbf{G}_\xi + \mathbf{H} = 0 \tag{1}$$

where

$$\mathbf{E} = h_2h_3\begin{vmatrix} \rho u \\ kp + \rho u^2 \\ \rho uv \\ \rho uw \end{vmatrix}, \quad \mathbf{F} = h_1h_3\begin{vmatrix} \rho v \\ \rho uv \\ kp + \rho v^2 \\ \rho vw \end{vmatrix},$$

$$\mathbf{G} = h_1h_2\begin{vmatrix} \rho w \\ \rho uw \\ \rho vw \\ kp + \rho w^2 \end{vmatrix}$$

$$\mathbf{H} = \begin{vmatrix} \rho uvh_3\dfrac{\partial h_1}{\partial \eta} + \rho uwh_2\dfrac{\partial h_1}{\partial \xi} - (kp + \rho v^2)h_3\dfrac{\partial h_2}{\partial \zeta} - (kp + \rho w^2)h_2\dfrac{\partial h_3}{\partial \zeta} \\ \rho uvh_3\dfrac{\partial h_2}{\partial \zeta} + \rho vwh_1\dfrac{\partial h_2}{\partial \xi} - (kp + \rho u^2)h_3\dfrac{\partial h_1}{\partial \eta} - (kp + \rho w^2)h_1\dfrac{\partial h_3}{\partial \eta} \\ \rho uwh_2\dfrac{\partial h_3}{\partial \zeta} + \rho vwh_1\dfrac{\partial h_3}{\partial \eta} - (kp + \rho u^2)h_2\dfrac{\partial h_1}{\partial \xi} - (kp + \rho v^2)h_1\dfrac{\partial h_2}{\partial \xi} \end{vmatrix}$$

ζ, η, and ξ are the independent variables, $k = (\gamma - 1)/2\gamma$, and h_1, h_2, and h_3 are the arcual derivatives (metric coefficients).

Equation (1) represents the continuity and three momentum equations in which pressure and density were made dimensionless with respect to freestream stagnation conditions, and velocity with respect to the maximum adiabatic velocity. Under the above assumptions the energy equation can be written in the following dimensionless form:

$$p = \rho(1 - q^2) \tag{2}$$

where

$$q^2 = u^2 + v^2 + w^2$$

Finite-Difference Scheme

The success of a numerical shock-capturing method in correctly predicting complicated flowfields depends on a proper formulation of the governing partial differential equations and a proper choice of the differencing scheme used to compute them. It is generally accepted by those who use these methods that success in predicting the proper location of a moving shock requires the use of differential equations that have been cast in divergence or conservative form as in Eq. (1). There appears, however, to be no general acceptance of a universal differencing scheme even when the order of numerical approximation is specified. A survey of various first- and second-order schemes[1] led the authors to conclude that first-order schemes are not acceptable for their purposes, and that of all second-order schemes proposed, the predictor-corrector combination proposed by MacCormack[2] is best. The criteria used to arrive at this judgment were ease of programming, required computing time, required machine storage, accuracy of results between shocks, and accuracy of locating the shocks and determining their intensity and definition. It is interesting that one of the principal proponents of sharp-shock techniques[3] also suggests that MacCormack's scheme is at least as good as any other second-order method for computing continuous portions of a flowfield.

In terms associated with studies devoted to the numerical integration of ordinary differential equations, MacCormack's method can be related to an Euler predictor followed by a modified Euler corrector; thus,

$$\tilde{u}_{n+1} = u_n + \Delta t u'_n \tag{3a}$$

$$u_{n+1} = u_n + \tfrac{1}{2}\Delta t(u'_n + \tilde{u}'_{n+1}) \tag{3b}$$

where Δt is a step size, and u'_n is the derivative of u_n which is a function of the single independent variable t. It is easy to see (but not often stated) that the second equation can also be written

$$u_{n+1} = \tfrac{1}{2}(u_n + \tilde{u}_{n+1} + \Delta t\tilde{u}'_{n+1}) \tag{3c}$$

and it is also evident that (in its implicit form) Eq. (3b) is basic to the well-known Crank-Nicolson integration technique often used for parabolic differential equations. If we apply Eqs. (3a) and (3c) to the simple, linear, hyperbolic equation

$$u_t + cu_x = 0 \tag{4}$$

we find

$$\tilde{u}_{n+1} = u_n - \Delta tc(u_x)_n \tag{5}$$

$$u_{n+1} = \tfrac{1}{2}[u_n + \tilde{u}_{n+1} - c\Delta t(\tilde{u}_x)_{n+1}]$$

MacCormack's method follows if the spatial derivative is replaced by a forward difference in the predictor and a backward difference in the corrector; thus, superscripting the time index n and introducing the space index j as a subscript

$$\tilde{u}_j{}^{n+1} = u_j{}^n - \nu(u_{j+1}{}^n - u_j{}^n) \tag{6}$$

$$u_j{}^{n+1} = \tfrac{1}{2}[u_j{}^n + \tilde{u}_j{}^{n+1} - \nu(\tilde{u}_j{}^{n+1} - \tilde{u}_{j-1}{}^{n+1})]$$

where $\nu = c\Delta t/\Delta x$ and is often referred to as the Courant number.

If MacCormack's scheme is used to difference Eq. (1),

$$\tilde{E}_{j,k^{n+1}} = E_{j,k^n} - (\Delta\zeta/\Delta\eta)(F_{j+1,k^n} - F_{j,k^n}) - (\Delta\zeta/\Delta\xi)(G_{j,k+1^n} - G_{j,k^n}) - H_{j,k^n}\Delta\zeta$$

$$E_{j,k^{n+1}} = \tfrac{1}{2}[E_{j,k^n} + \tilde{E}_{j,k^{n+1}} - (\Delta\zeta/\Delta\eta)(\tilde{F}_{j,k^{n+1}} - \tilde{F}_{j-1,k^{n+1}}) - (\Delta\zeta/\Delta\xi)(\tilde{G}_{j,k^{n+1}} - \tilde{G}_{j,k-1^{n+1}}) - \tilde{H}_{j,k^{n+1}}\Delta\zeta] \quad (7)$$

where $E_{j,k^n} = E(n\Delta\zeta, j\Delta\eta, k\Delta\xi)$ and F_{j,k^n}, G_{j,k^n}, H_{j,k^n} represent $F(E_{j,k^n})$, etc. Several variations of the scheme are apparent and follow from interchanges of the forward and backward space differences. Simple tests[1] show that these different forms give slightly different results, depending upon the direction in which the shock is traveling within the mesh. A forward difference in the predictor should be used, if possible, with a forward-moving shock. To remove this preferential behavior, the forward-backward order of the space differencing can be cyclically permuted as n increases.

Cone at Angle of Attack

When the angle of attack of a cone in a supersonic flowfield is increased such that supersonic crossflow velocities result, embedded shock waves may form on the lee side of the cone. This problem, although involving multishocks, poses no special difficulty for a shock-capturing technique.

The problem concerning a cone at small incidence is not new. Early solutions[8-11] involved several simplifying assumptions, which sometimes yielded analytical solutions. However, the assumptions imposed were sometimes not justified, and the error introduced could not as a rule be determined. More recent numerical solutions,[12-18] in which the angle of attack is on the order of the cone half-angle, were found using a finite-difference approach in conjunction with a shock fitting procedure. None, however, found embedded shock waves.

The method of solution used here will be described briefly. Equation (1) is cast into the body-oriented coordinate system shown in Fig. 1 in which x lies along the body, y is perpendicular to the body, and ϕ is the meridional angle. Body coordinates are chosen to facilitate the addition of a nonconical afterbody. The metric coefficients for this system are $h_1 = 1 + y/R_b$, $h_2 = 1$, $h_3 = r$ where R_b is the lengthwise radius of curvature of the body and r is the cylindrical radius. Substituting this information into Eq. (1), and setting $R_b = \infty$, results in the governing set of partial differential equations to be solved. A finite-difference network is set up in the (y,ϕ) plane in which Δy and $\Delta\phi$ are constant. In the y direction the mesh begins one mesh point inside the body ($y = -\Delta y$ or $j = 1$) and extends to a point well into the freestream ($y = y_{\max}$ or $j = NY2$). Since there is a plane of symmetry in this problem, it is only necessary to determine the flowfield on one side of the cone. Thus, in the ϕ direction the mesh begins at $\phi = -\Delta\phi(k = 1)$ and terminates at $\phi = 180° + \Delta\phi$ $(k = N\phi 3)$.

The initial conditions are supplied by using the values of the flow variables in the freestream for the entire grid. Boundary conditions at the body are that the normal component of velocity is zero and all the remaining dependent variables are reflected (i.e., are assumed to be locally even functions with respect to the body). No attempt was made to resolve the entropy layer associated with conical flow. The partial differential equations are differenced and then integrated numerically from $x = 1$ to $x = 2$ at which time under the conical flow assumption, the distance between the shock and the body will have doubled. The flow variables are then "stepped back" to $x = 1$ by taking the values at every other point in an array computed at $x = 2$ and feeding them back consecutively into an array for $x = 1$. Only the lower half of the mesh points at $x = 1$ are reinitialized by this procedure. The rest are assigned freestream values. This entire procedure is repeated cyclically until there is little change between the flow variables at $x = 2$ for two subsequent cycles, at which time the solution is assumed to have converged.

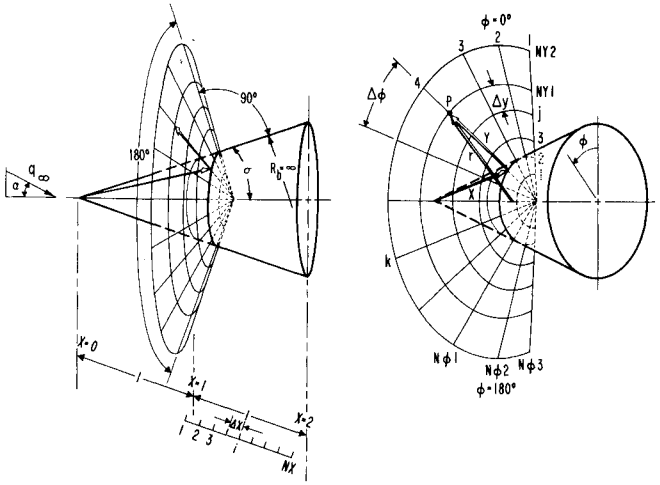

Fig. 1 Coordinate system and mesh description for cone.

Computational results were obtained which describe the flowfield about a 10° half-angled cone in Mach 5 flow for angles of attack from 0° to 15°. To demonstrate the ability of the shock-capturing technique to predict the flowfield accurately about a cone, the meridional surface pressure distribution for the 5° angle-of-attack case is compared in Fig. 2 with the results of Babenko[13] who used a 20 by 16 grid, Jones[17] who used a 10 by 8, and Moretti[18] who used a 6 by 10. The computations using the shock-capturing technique were performed using first a 16 by 10 and then a 32 by 20 grid with no apparent difference in the solutions. The computation time for the 16 by 10 grid case was approximately 2 min on an IBM 360/67 linked with the CRT. Results are also compared with those of Babenko for the 0°, 2.5°, and 7.5° cases in Fig. 2. The agreement is excellent. It should also be mentioned that the location and intensity of the shock wave were predicted quite accurately by the present method. As the angle of attack is increased, it is observed that at 12° a weak embedded, crossflow shock wave begins to form near the 155° meridional plane. As the angle of attack is increased further to 14° and then 15°, it intensifies and thus becomes more clearly defined.

Nonconical Bodies

In this section a shock-capturing technique is used to determine the supersonic flowfield above and behind pointed

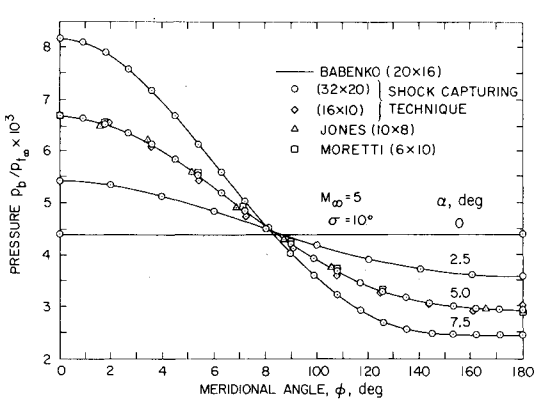

Fig. 2 Comparison of surface pressure distributions with sharp-shock theories.

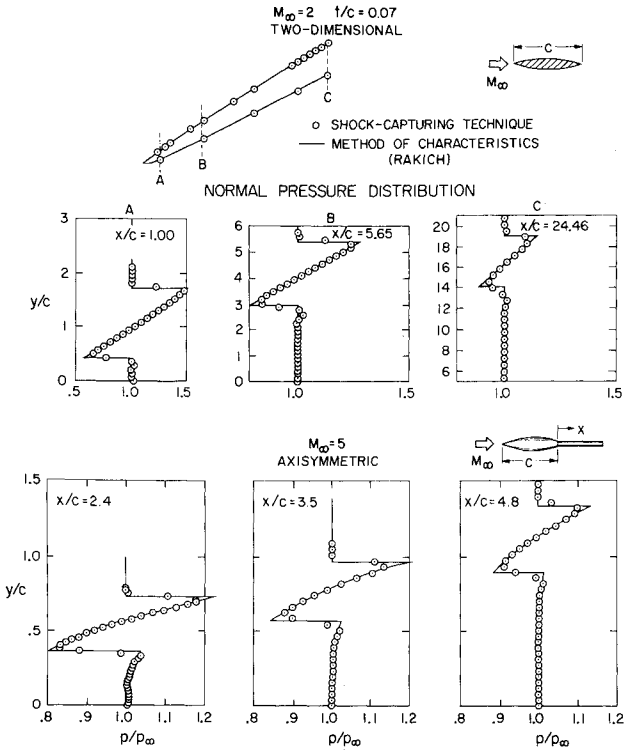

Fig. 3 Shock shapes and normal pressure distributions for two-dimensional and axisymmetric bodies.

ogives (both two-dimensional and axisymmetric) and cone-cylinders at zero incidence. The object of this study was to determine how well this technique predicted the location and intensity of attached and embedded secondary shock waves when used as a marching ahead technique similar to the method of characteristics. The computational results obtained, when possible, are compared with experiment and the method of characteristics. The same body-oriented coorinate system is used here as was used in the cone at angle-of-attack problem. The difference between the two problems is in the equation describing the variation of the cylindrical radius, r, with distance along the body, and the radius of curvature of the body, R_b.

Since the angle of attack is zero, the flow is axisymmetric, and it is only necessary to set up a grid in the y direction or in the direction normal to the body. For the pointed ogive the exact shape was assumed to be a circular arc afterbody with either a wedge-shaped or cone-shaped nose. For both the pointed ogive and the cone-cylinder, the integration begins at the transition point between the cone and the afterbody. The initial data for the flow variables in the grid are supplied, therefore, by using a converged solution generated by the cone program of the previous section.

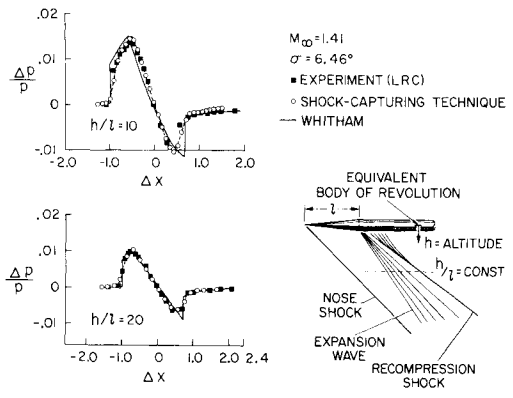

Fig. 4 "N"-waves generated by cone-cylinder.

For this particular problem three different approaches are tried for numerically simulating the surface boundary conditions. The first scheme simply makes use of the reflection principle in which pressure, density, and the tangential velocity are assumed locally to be even functions with respect to the body, while the normal velocity is assumed locally to be an odd function. The second scheme entails a local application of the method of characteristics. Since the governing set of partial differential equations is hyperbolic, there exists a corresponding set of characteristics which can be used to determine the flow conditions on the body from field data just above the body.[18] The third approach is similar to that used in the cone problem. The pressure at the body is determined using the reflection principle, while the density and tangential velocity are determined from the constant entropy assumption at the body. It should be pointed out that the second and third approaches are not applicable during the formation of an attached secondary shock because constant entropy was assumed in their development. It was found that the surface pressure and density distributions obtained for moderately curved bodies did not differ significantly for the three different boundary condition schemes.

In order to approximate the method of characteristics as closely as possible (satisfy the shift condition[4]), it is desirable to use the largest possible step size while still maintaining a stable solution. The stability criteria for MacCormack's method based on the associated amplification matrix is

$$\Delta x/\Delta y \leq \text{const}/|\sigma_{\max}| \tag{8}$$

where const = 1 and $\sigma_{\max}$ is the maximum eigenvalue of the coefficient matrix of the gasdynamic equations, and is given by the following equation for body coordinates:

$$\sigma_{\max} = \mathcal{H}\{[|uv| + c(u^2 + v^2 - c^2)^{1/2}]/(u^2 - c^2)\} \tag{9}$$

where $\mathcal{H} = 1 + y/R_b$ and c is the local speed of sound. Preliminary experimentation seems to indicate that Eqs. (8) and (9) predicted a larger step size than was actually possible. Plots of the actual and theoretical maximum allowable step sizes varied only by a constant, generally slightly below unity. The optimum step size that would yield the best possible solution could therefore be predicted.

With a fixed mesh system it is possible for the maximum eigenvalues to occur anywhere in the flowfield, including the freestream. It is interesting that when the maximum eigenvalue occurred in the vicinity of the leading edge or bow shock, such as in the case with the pointed ogive, the constant in Eq. (8) was less than unity (0.98). However, when the maximum eigenvalue occurred within the shock layer, for example in the expansion region surrounding a cone-cylinder, the constant was unity. This meant that at that point in the flowfield the shock-capturing technique was identical to the method of characteristics.

Because of the coordinate system chosen for this problem, the leading-edge shock wave moves upward throughout the fixed mesh as the integration proceeds downstream. When the leading-edge shock approaches the upper boundary of the mesh, the value of Δy (the distance between two mesh points) is doubled, and the flow variables at every other mesh point are discarded. This procedure has an apparent smoothing behavior, but no appreciable loss in accuracy is incurred by using it.

The ability of a shock-capturing technique to predict the location and intensity of secondary shocks is demonstrated by the results shown in Figs. 3 and 4. Figure 3 shows the pressure distribution along vertical lines at various stations behind the body, and both leading and trailing-edge shocks for a circular arc airfoil in Mach 2 flow. It also shows similar pressure distributions behind a pointed ogive in Mach 5 flow. Both cases are compared with solutions computed by the method of characteristics.[15] For both the two-dimensional

and axisymmetric flowfields the locations of the shock waves are predicted quite accurately by the shock-capturing technique. However, the peak overpressure of the waves is somewhat dissipated, this being a predictable effect of the numerical method.

Figure 4 shows typical "N"-waves obtained 10 and 20 body lengths below a cone-cylinder in Mach 1.41 flow. The results are compared with Whitham's theory and also with the experimental results of Carlson.[19] The location and intensity of both shocks agree well with experiment but vary somewhat from Whitham's theory. For this particular case, it took approximately 2.5 min on the 360/67 to integrate 20 body lengths downstream for a 200-point grid in the y direction.

Conical Wing-Body Combination

The ability of shock-capturing techniques to correctly predict flowfields which contain complicated shock and expansion wave patterns offers a new tool to the aerodynamicist who is interested in determining surface forces and near field effects as a result of the nonlinearity of the equations about supersonic aircraft. In this section the compression side of the flowfield about a conical wing-body combination at angle of attack is determined (Fig. 5). The conical body and planar delta wing combine to yield favorable interference effects by increasing the maximum lift-drag ratio. The optimum configuration is obtained when the wing's leading edge and the shock generated by the body intersect. This particular configuration is also of interest because the flowfield generated about it can be used as a starting solution for more complicated, nonconical configurations.

A spherical coordinate system is chosen because it is conformal for the conical wing-body combination; i.e., the body lies parallel to two of the coordinate directions. The metric coefficients for this system are $h_1 = 1$, $h_2 = r$, and $h_3 = r \sin\theta$, and when substituted into Eq. (1) yield the form of the equations to be differenced. Since there exists a plane of symmetry and the wing's leading edge is assumed supersonic, it is only necessary to solve for one-quarter of the entire flowfield. The flowfield is discretized in the (θ,ϕ) plane. The meridional plane in which the wing is located can be varied to effect a change in the dihedral of the wing. The gas-dynamic equations are then integrated cyclically from $r = 1$ to $r = 1 + \Delta r$ until there is little change in the flow variables, thus establishing a conical flow.

In order to determine the effects of positive and negative dihedral on the resulting flowfield, a 5.7° half-angled cone with a planar delta wing was computed at 4.6° angle of attack in Mach 6 flow. The wing angle was varied in order to keep the body shock coincident with the wing's leading edge. The surface pressure distributions for the 0° and ±5° dihedral cases are shown in Fig. 6. The results obtained for the 0° case are compared with the approximate theory of Savin.[20] For the 5° dihedral case the surface pressure distribution is found to decrease over the entire body when compared to the 0° dihedral case, and it is necessary to increase the wing angle (decrease the sweep) in order to keep the body shock coincident with the leading edge. The −5° dihedral case has the opposite effect.

The present theory and experiment[21] are compared in Fig. 7 for a 12.5° half-angled cone with a 65° swept delta wing in Mach 5.08 flow. The point of intersection of the body shock with the wing predicted by theory for the $\alpha = 0°$ case varied somewhat from the experiment. Some of this variance is believed to be a result of shock, boundary-layer interaction effects. However, the surface pressure coefficients for both angles of attack agree well with the experiment. For the problems solved in this study a 30 by 11 mesh was used. Each calculation required approximately 15 min of computer time on the IBM 7094 computer system.

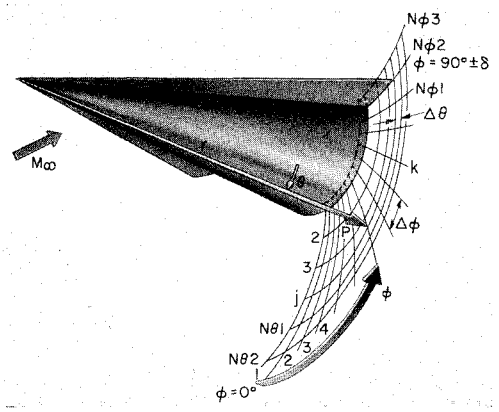

Fig. 5 Coordinate system and mesh description for conical wing-body combination.

Delta Wing

The supersonic flowfield surrounding a lifting delta wing with supersonic leading edges has been the object of many theoretical and experimental studies in the past. The purpose in this section is first to determine the flowfields on both the compression and expansion sides of a planar delta wing, and second to combine these two solutions at the trailing edge forming an initial data plane which can be integrated downstream to give the inviscid flow in the wake of the delta wing.

Compression side calculations have been made by such investigators as Fowell,[22] South and Klunker,[23] Babaev,[24] Beeman and Powers,[25] and Voskresenskii.[26] The flowfield on this side of the delta wing poses no great problem for the sharp-shock techniques used by these investigators, and they obtain comparable results. The computational region is bounded by the body and by the attached bow shock.

Expansion side calculations have been attempted by Fowell,[22] Babaev,[27] and Beeman and Powers.[25] This flowfield is somewhat more complicated than the compression side since at some distance inboard of the leading edge an embedded shock wave is produced as a result of the supersonic crossflow velocities. Babaev in his computations accounted for the embedded shock wave but somehow failed to predict the correct values of the flow variables in the constant flow region between this shock wave and the leading edge. Beeman and Powers, in their method of characteristics program, ran into difficulty in fitting the embedded shock and simply assumed it to be an isentropic compression, resulting in dislocation of the embedded shock.

In the past no attempt has been made to determine the complete inviscid flowfield in the wake of a lifting delta wing.

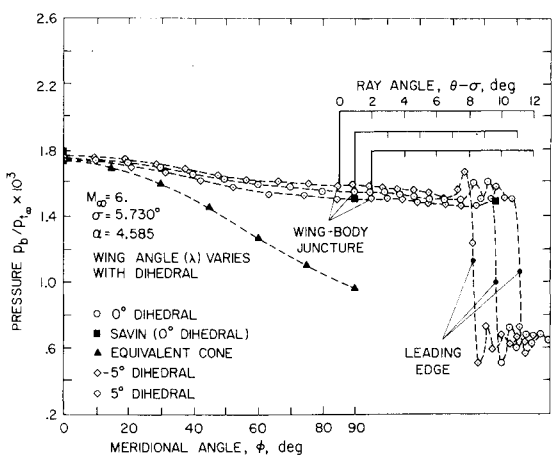

Fig. 6 Variation of surface pressure distribution with wing dihedral for wing-body combination.

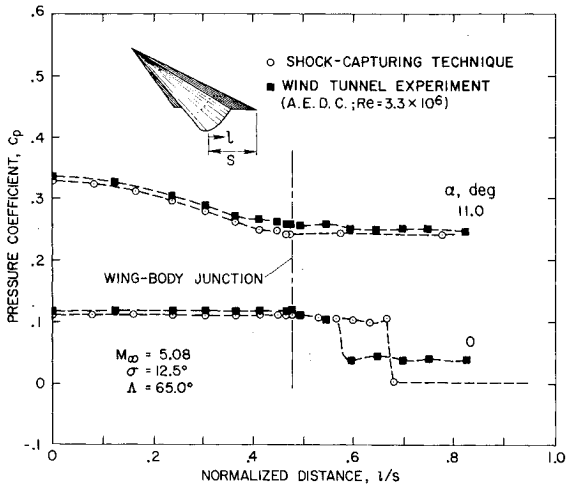

Fig. 7 Comparison of shock-capturing technique with experiment for conical wing-body combination.

The flowfield is not only complicated by the existing compression and expansion side flowfields, containing various combinations of shock and expansion waves, but also by the newly generated trailing-edge shock and expansion waves. This class of problems is a good test for the usefulness of shock-capturing techniques.

As in the problems discussed previously, the boundary conditions helped dictate the choice of the coordinate system. Orienting the wing in the Cartesian system shown in Fig. 8 in which the axis of the wing coincides with the x axis and the surface of the wing lies in the (x,z) plane, one can define the conical coordinates, normalized with respect to the tangent of the wing angle β as follows:

$$\zeta = x, \quad \eta = y/(x \tan\beta), \quad \xi = z/(x \tan\beta) \tag{10}$$

where $\eta = 0$ corresponds to the plane of the wing, $\xi = 0$ to the plane of symmetry, and $\xi = 1$ to the wing's leading edge.

Using this nonorthogonal coordinate transformation on the Cartesian form of Eq. (1), one finds the following equation:

$$\mathbf{E}'_\zeta + \mathbf{F}'_\eta + \mathbf{G}'_\xi + \mathbf{H}' = 0 \tag{11}$$

where

$$\mathbf{E}' = \zeta\mathbf{E}, \quad \mathbf{F}' = (\mathbf{F}/\tan\beta) - \eta\mathbf{E},$$
$$\mathbf{G}' = (\mathbf{G}/\tan\beta) - \xi\mathbf{E}, \quad \text{and} \quad \mathbf{H}' = \mathbf{E}$$

The integration of Eq. (11) is performed with respect to ζ, since the equation is hyperbolic with respect to that coordinate. The flow variables p, ρ, u, v, and w are, therefore, determined from the conservative variables $\mathbf{E}'$. This necessitates the solution of the following five simultaneous, algebraic equations:

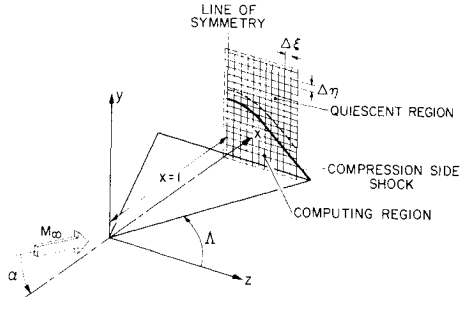

Fig. 8 Coordinate system and mesh description for delta wing.

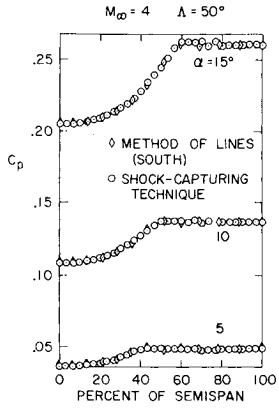

Fig. 9 Spanwise pressure distribution on compression side of planar delta wing.

$$E_1' = a = \zeta\rho u, \quad E_2' = b = \zeta(kp + \rho u^2)$$
$$E_3' = c = \zeta(\rho uv), \quad E_4' = d = \zeta(\rho uw) \tag{12}$$
$$p = \rho(1 - u^2 - v^2 - w^2)$$

where a, b, c, and d are known after each integration step.

The solution of these five equations is:

$$v = c/a, \quad w = d/a$$
$$u = [-B + (B^2 - 4AC)^{1/2}]/2A \tag{13}$$

where

$$A = 1 - k, \quad B = -b/a, \quad C = k(1 - v^2 - w^2)$$
$$\rho = a/\zeta u, \quad p = \rho(1 - u^2 - v^2 - w^2)$$

The positive sign appearing before the radical in Eq. (13) is used because u (the ζ component of velocity) is supersonic throughout the entire field of integration.

The procedure for determining the conical flowfields on the windward and leeward sides of the delta wing is similar to that used in the conical wing-body problem. Equation (11) is integrated cyclically from $\zeta = 1$ to $\zeta = 1 + \Delta\zeta$ until conical flow is established for the boundary conditions imposed. Plane of symmetry boundary conditions are applied at the left-hand boundary (see Fig. 8) of the mesh since the flowfield is symmetrical to it. The uppermost part of the mesh is chosen such that it remains entirely in the freestream, and the boundary conditions there are fixed accordingly. Exact boundary conditions are applied at the right-hand side since these can be computed from the oblique-shock or Prandtl-Meyer relations which apply along supersonic leading edges. Two types of boundary conditions were tried at the wing surface; both required that the normal component of velocity be zero, one used the reflection principle for all of the remaining dependent variables, and the other applied in addition a constancy of entropy where appropriate. The results indicate that the simple use of the reflection principle is adequate throughout.

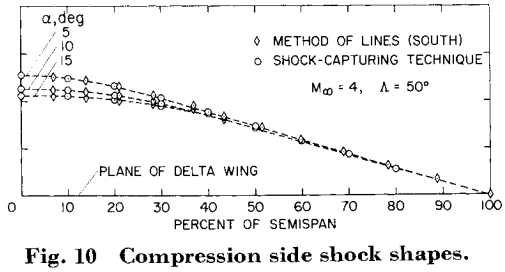

Fig. 10 Compression side shock shapes.

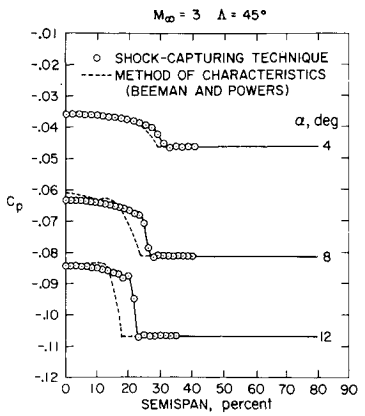

Fig. 11 Spanwise pressure distribution on expansion side of planar delta wing.

For both the compression and expansion side calculations, initial conditions are supplied by using the values of the flow variables in the freestream. Initially most of the grid points are at freestream conditions, and it is not really necessary to difference these undisturbed points. Therefore, a check is coded into the program to see how far from the body a disturbance has propagated, and a "freeze-out" is imposed on the integration of the points above this disturbance. This procedure saves as much as 30% in computing time.

After the complete flowfield is determined on both sides of the delta wing, the two solutions are combined at the trailing edge to form an initial data plane for which Eq. (11) can then be numerically integrated downstream through the wake. In this case the only boundary condition imposed is that the freestream exist along all edges of the mesh where symmetry does not apply.

A simple stability analysis based on the amplification matrix can be performed to yield ratios of step size to mesh interval in each direction for the conical coordinate system. These ratios are defined by the following equations:

$$\Delta\zeta/\Delta\eta = \zeta \text{ const}/(|\sigma_{\max_1}/\tan\beta| + |\eta_{\max}|) \qquad (14)$$

where

$$\sigma_{\max_1} = [|uv| + c(u^2 + v^2 - c^2)^{1/2}]/(u^2 - c^2)$$

and

$$\Delta\zeta/\Delta\xi = \zeta \text{ const}/(|\sigma_{\max_2}/\tan\beta| + |\xi_{\max}|) \qquad (15)$$

where

$$\sigma_{\max_2} = [|uw| + c(u^2 + w^2 - c^2)^{1/2}]/(u^2 - c^2)$$

Dividing Eq. (15) by Eq. (14) will give the optimum mesh ratio $(\Delta\eta/\Delta\xi)$, based on local linear theory.

Equations (14) and (15) indicate that any instability should occur where η and ξ are maximum. For this particular problem this should occur in the freestream. Experimental stability studies do, in fact, show evolving instabilities in the region undisturbed by the body. When freeze-out is used, the onset of an instability is forced into the disturbed region and a larger step size is therefore possible. For a compression side calculation Eq. (14) was used to govern the step size. The strong shock that formed usually varied little in intensity along its length, and therefore, appeared to be quite sharp. It was therefore not critical to use the optimum mesh ratio $(\Delta\eta/\Delta\xi)$ in the vicinity of the shock wave. However, in performing an expansion side calculation which entailed capturing a weak embedded shock, it was necessary to use the optimum mesh ratio $(\Delta\eta/\Delta\xi)$ in order to obtain a sharply defined shock wave. In computing the wake flow, some sacrifice in resolution of the embedded shock wave had to be made in order to use the same mesh ratio for both compression and expansion side calculations.

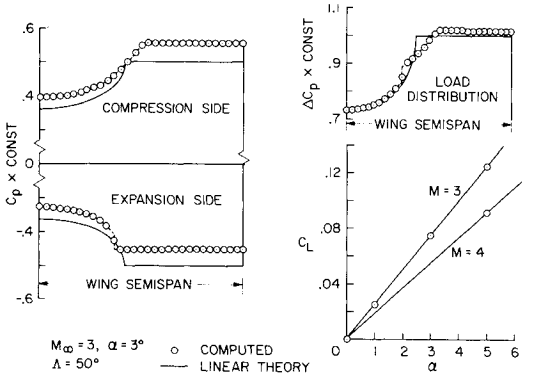

Fig. 12 Pressure and load distribution on planar delta wing.

Computations were performed to determine the flowfield over the compression side of a 50° swept, planar delta wing. Figure 9 shows the results of those computations for angles of attack of 5°, 10°, and 15° at Mach 4. The semispan pressure distributions are compared with the results of South and Klunker[23] who used a method of lines technique (sharp shock). South in turn made comparisons with Voskresenskii[22] and found good agreement, and with Babaev[24] and found poor agreement. The present results substantiate South's good comparison with Voskresenskii. Figure 10 shows a comparison of the shock shapes for the above flow conditions. There is very little disagreement with South's results. The shock shape obtained using the shock-capturing technique was located using a weighted gradient technique coded into the program.

The surface pressure coefficient on the expansion side of a 45° swept delta wing in Mach 3 flow for 4°, 8°, and 12° angle of attack is shown in Fig. 11. The results are compared with a method of characteristics technique devised by Beeman and Powers,[22] who chose to neglect the weak crossflow shock, assuming instead an isentropic compression. The disagreement in the location of the embedded shock is believed to be the result of their assumption. However, the pressure distributions on either side of the shock are in good agreement. The grid size used for these problems consisted of 34 points normal to the body and 26 points parallel to the body, and computation times were on the order of 10 min on the 360/67.

The results obtained for the compression and expansion side flowfields of a 50° swept delta wing at 3° angle of attack in Mach 3 flow are compared with linear theory in Fig. 12. It is interesting that although there is considerable disagreement between the two theories for the individual surface pressure distributions and a slight disagreement in the load distribution, there is almost no variation in the plot of lift coefficient vs angle of attack.

The complete inviscid flowfield in the wake of a 55° swept, planar delta wing at 1.8° angle of attack in Mach 2.7 flow was determined after having first determined the compression and expansion side flowfields. The results of this calculation

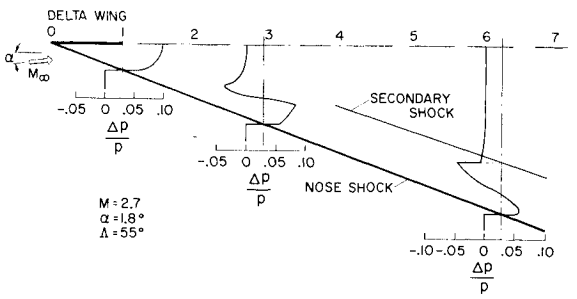

Fig. 13 Windward, centerline pressure distributions beneath planar delta wing.

which were displayed in movie form clearly show the formation of the trailing-edge shock wave on the leeward side and expansion wave on the windward side. The formation of the secondary recompression shock on the windward side is also clearly recognizable. Figure 13 shows the plane of symmetry compression side shock locations, and normal pressure distributions between the plane of the wing and the free-stream at various stations downstream. The pressure curves shown were faired through the numerical data, and the actual shock waves did not appear as sharp discontinuities but were spread over two mesh intervals.

All results shown for the wake flow were obtained from an integration of the full Eulerian equations over a 68 by 32 mesh. About 30 min of CPU time on an IBM 360/67 were required to carry the solution from the trailing edge to 33 chord lengths behind it. The calculations were monitored from a CRT, and instabilities were suppressed when they appeared by modifying the advancing step size directly through the CRT interface. This increased the real time computation to about 40 minutes without significantly increasing CPU time.

Conclusions

A case has been presented for the reliability of a second-order, shock-capturing numerical technique based on the predictor-corrector differencing scheme proposed by MacCormack. It has been demonstrated that this approach is capable of handling complicated, multishocked flows and would therefore lend itself to the solution for flowfields over quite complicated configurations. It has been shown to yield good results in comparison with other applicable methods and with experiments in which viscous effects are not predominant. These comparisons are presented for simple body shapes, triangular wings, and simple triangular wing-body combinations. Extensions to wings with camber and thickness as well as nonconical bodies with attached wings are obvious eventualities. Immediate applications, are possible in the area of near field sonic boom definition for which the use of a shock-capturing technique should prove to be of considerable value.

References

[1] Kutler, P., "Application of Selected Finite Difference Techniques to the Solution of Conical Flow Problems," Ph.D. thesis, Dept. of Aerospace Engineering, 1969, Iowa State Univ., Ames, Iowa.

[2] MacCormack, R. W., "The Effect of Viscosity in Hypervelocity Impact Cratering," AIAA Paper 69-354, Cincinnati, Ohio, 1969, pp. 1–7.

[3] Moretti, G., "The Choice of a Time-Dependent Technique in Gas Dynamics," PIBAL 69-26, 1969, Polytechnic Inst. of Brooklyn.

[4] Kutler, P. and Lomax, H., "The Computation of Supersonic Flow Fields About Wing-Body Combinations by 'Shock-Capturing' Finite Difference Techniques," *Second International Conference on Numerical Methods in Fluid Dynamics*, Sept. 1970; also *Lecture Notes in Physics*, Vol. 8, 1971, pp. 24–29.

[5] Richtmyer, R. D. and Morton, K. W., *Difference Methods for Initial-Value Problems*, Wiley, New York, 1967.

[6] Rusanov, V. V., "On Difference Schemes of Third Order Accuracy for Nonlinear Hyperbolic Systems," *Journal of Computational Physics*, Vol. 5, 1970.

[7] Burstein, S. Z. and Mirin, A. A., "Third Order Difference Methods for Hyperbolic Equations," *Journal of Computational Physics*, Vol. 5, 1970.

[8] Ferri, A., "Supersonic Flow Around Circular Cones at Angles of Attack," TN 2236, 1951, NASA.

[9] Stocker, P. M. and Mauger, F. E., "Supersonic Flow Past Cones of General Cross-Section," *Journal of Fluid Mechanics*, Vol. 13, 1962, pp. 383–399.

[10] Kopal, Z., "Tables of Supersonic Flow Around Cones," TR 1, 1947, Dept. of Electrical Engineering, Center of Analysis, MIT, Cambridge, Mass.

[11] Melnik, R. E., "Vortical Singularities in Conical Flow," *AIAA Journal*, Vol. 5, No. 4, April 1967, pp. 631–637.

[12] Emery, A. F., "An Evaluation of Several Differencing Methods for Inviscid Fluid Flow Problems," *Journal of Computational Physics*, Vol. 2, 1968, pp. 306–331.

[13] Babenko, K. I., Voskresenskii, G. P., Lyubimov, A. N., and Rusanov, V. V., "Three-Dimensional Flow of Ideal Gas Past Smooth Bodies," TT F-380, 1966, NASA.

[14] Gonidou, R., "Supersonic Flows Around Cones at Incidence," TT F-11, 1968, p. 473, NASA.

[15] Rakich, J. V. and Cleary, J. W., "Theoretical and Experimental Study of Supersonic Steady Flow Around Inclined Bodies of Revolution," AIAA Paper 69-187, New York, 1969, pp. 1–9.

[16] Holt, M., and Ndefo, D. E., "A Numerical Method for Calculating Steady Unsymmetrical Supersonic Flow Past Cones," *Journal of Computational Physics*, Vol. 5, 1970, pp. 463–486.

[17] Jones, D. J., "Numerical Solutions of the Flow Field for Conical Bodies in a Supersonic Stream," LR-507, 1968, National Research Council of Canada.

[18] Moretti, G., "Inviscid Flow Field Past a Pointed Cone at an Angle of Attack," TR 577, 1965, General Applied Science Labs.

[19] Carlson, H. W., Mack, R. J., and Morris, O. A., "A Wind-Tunnel Investigation of the Effect of Body Shape on Sonic-Boom Pressure Distributions," TN D-3106, 1965, NASA.

[20] Savin, R. C., "Approximate Solutions for the Flow About Flat-Top Wing Body Configurations at High Supersonic Airspeeds," RM A58F02, 1958, NACA.

[21] Randall, R. E., Bell, D. R., and Burk, J. L., "Pressure Distribution Test of Several Sharp Leading Edge Wings, Bodies, and Body-Wing Combinations at Mach 5 and 8," TN 60-173, 1960, Arnold Engineering Development Center, Tullahoma, Tenn.

[22] Fowell, L. R., "Exact and Approximate Solutions for the Supersonic Delta Wing," *Journal of the Aeronautical Sciences*, Vol. 23, 1956.

[23] South, J. C. and Klunker, E. B., *Methods for Calculating Nonlinear Conical Flows*, NASA, SP-228, 1969, pp. 131–158.

[24] Babaev, D. A., "Numerical Solution of the Problem of Supersonic Flow Past the Lower Surface of a Delta Wing," *AIAA Journal*, Vol. 1, No. 9, Sept., 1963, pp. 2224–2231.

[25] Beeman, E. R. and Powers, S. A., "A Method for Determining the Complete Flow Field Around Conical Wings at Supersonic/Hypersonic Speeds," AIAA Paper 69-646, San Francisco, Calif., 1969.

[26] Voskresenskii, G. P., "Numerical Solution of the Problem of a Supersonic Gas Flow Past an Arbitrary Surface of a Delta Wing in the Compression Region," *Izvestya Akademiaa Nauk SSSR, Mekh. Zhidk. Gaza*, No. 4, 1968, pp. 134–142.

[27] Babaev, D. A., "Numerical Solution of the Problem of Flow Round the Upper Surface of a Triangular Wing by a Supersonic Stream," *Zhurnal vychislitel'noi matematiki i matelmaticheskoi fizika*, Vol. 2, 1962, pp. 278–289.